

Pseudointegrable Andreev billiard

Jan Wiersig*

Max-Planck-Institut für Physik komplexer Systeme, D-01187 Dresden, Germany

(Received 25 June 2001; published 1 March 2002)

A circular Andreev billiard in a uniform magnetic field is studied. It is demonstrated that the classical dynamics is pseudointegrable in the same sense as for rational polygonal billiards. The relation to a specific polygon, the asymmetric barrier billiard, is discussed. Numerical evidence is presented indicating that the Poincaré map is typically weak mixing on the invariant sets. This link between these different classes of dynamical systems throws some light on the proximity effect in chaotic Andreev billiards.

DOI: 10.1103/PhysRevE.65.036221

PACS number(s): 05.45.-a, 74.50.+r

I. INTRODUCTION

Billiards have played a prominent role in the understanding of classical and quantum mechanics. In such a system, a particle moves freely in a domain with specular reflections at the boundary (the angle of reflection equals the angle of incidence); see, e.g., [1]. Billiards of a different kind are realized in ballistic mesoscopic samples connected to a superconductor [2,3]. The boundary of such an *Andreev billiard* [4] consists of normal-conducting regions with specular reflections and superconducting regions with Andreev reflections, whereby electronlike quasiparticles with charge $-q$, mass m , and energy ε above the Fermi energy in the normal metal are retroreflected as holelike quasiparticles with charge q , mass $-m$, and energy $-\varepsilon$. In the absence of a magnetic field, retroreflected orbits are self-retracing and, therefore, periodic. The presence of a magnetic field allows for a richer spectrum of dynamical behavior [4].

In this paper, we study an interesting Andreev billiard, the circular Andreev billiard in a uniform magnetic field. Our analysis will lead one to the conclusion that boundary points separating normal and superconducting regions, henceforth called *critical points*, have the same consequences on the classical dynamics as *critical corners* in rational polygonal billiards. In such a polygon, all angles $\alpha_j = m_j \pi / n_j$ between sides are rationally related to π , where $m_j, n_j > 0$ are relatively prime integers. The free motion inside a rational polygon is characterized as *pseudointegrable* [5] since it shares some properties of integrable systems: (i) the phase space is foliated by two-dimensional invariant surfaces [6,7]; (ii) the flow on these surfaces is ergodic and not mixing [8], and, in particular, not chaotic (see, e.g., [9] for the definition of ergodic properties). Yet, in the presence of critical corners with $m_j > 1$ the dynamics is more complex: (i) the genus of the surfaces is greater than one [5]; (ii) the dynamics is not quasiperiodic; and (iii) presumably weak mixing, but this is proven only for a special subclass; see, e.g., [8]. Numerical evidence for weak mixing has been reported in [10,11].

The paper is organized as follows. In Sec. II, we introduce the circular Andreev billiard and derive its Poincaré map, which describes the collision-to-collision discrete dynamics. We show that the dynamics is pseudointegrable, in the same

sense as for rational polygons. The relation to the asymmetric barrier billiard is discussed in Sec. III. Section IV presents numerical evidence that the Poincaré map is typically weak mixing on the invariant sets. In Sec. V, we draw conclusions and give an outlook.

II. THE CIRCULAR ANDREEV BILLIARD

Let us first consider the conventional circular billiard in a magnetic field with strength B directed perpendicular to the plane. The classical motion of a particle with mass m , charge q , and speed v confined inside a circle with specular reflections is integrable; see Ref. [12] and references therein. The orbits consist of a series of arcs of circles with the Larmor radius $R = mv/(qB)$. Without loss of generality, we scale the radius of the billiard and the absolute value of the momentum to unity. If $R < 1$, some orbits form complete circles entirely inside the boundary. Ignoring these complete circles, we can specify each orbit by giving the sequence of its positions and directions immediately after each impact at the boundary. The position on the circular boundary is parametrized by the arclength $\phi \in [0, 2\pi)$. The direction of the orbit after impact is labeled by the angle of reflection $\alpha \in [0, \pi]$, or by the tangential momentum $p = \cos \alpha \in [-1, 1]$. Elementary geometry depicted in Fig. 1 gives the Poincaré

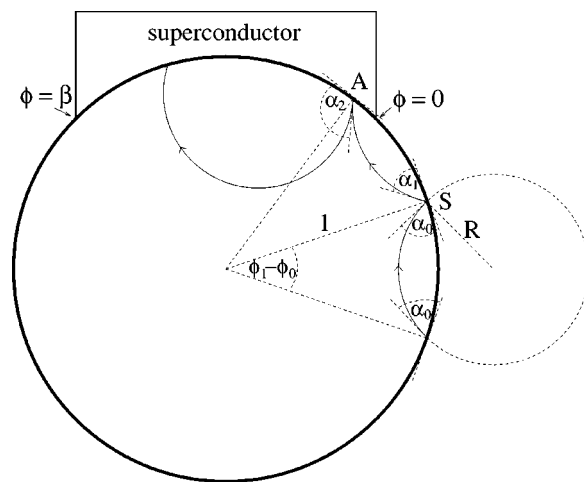


FIG. 1. Part of a typical trajectory (solid arcs of circles) with specular (S) and Andreev (A) reflections in the circular Andreev billiard. Dashed lines serve for the construction of maps (1)–(6).

*Email address: jwiersig@mpipks-dresden.mpg.de

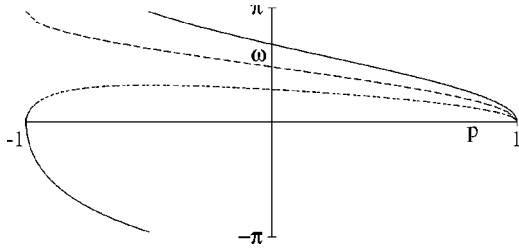


FIG. 2. ω as function of p according to Eq. (3) with $R > 1$ (solid), $R = 1$ (dashed), and $R < 1$ (dotted). The lines $\omega = \pi$ and $\omega = -\pi$ are identified.

map, i.e., the discrete bounce map from the n th to the $(n + 1)$ th collision with the boundary

$$\phi_{n+1} = \phi_n + \omega(p_n) \pmod{2\pi}, \quad (1)$$

$$p_{n+1} = p_n, \quad (2)$$

with

$$\omega(p) = 2 \arctan\left(\frac{R\sqrt{1-p^2}}{1+Rp}\right); \quad (3)$$

modulo 2π restricts the variable to the interval $[0, 2\pi)$. The function $\omega(p)$ is illustrated in Fig. 2. Note the broken time-reversal symmetry, $\omega(-p) \neq -\omega(p)$.

The properties of the maps (1) and (2) are related to the continuous-time evolution in a simple manner: conservation of p corresponds to conservation of angular momentum; ergodic motion on an invariant circle $p = \text{const}$ for irrational ω is related to ergodic motion on a two-dimensional invariant torus; families of fixed points for rational ω correspond to resonant tori foliated by periodic orbits.

The situation with a superconducting interface at $\phi \in (0, \beta)$ is illustrated in Fig. 1. For simplicity, let us first assume that the quasiparticles are exact at the Fermi energy, i.e., $\varepsilon = 0$. An Andreev reflection at the interface is then just a change of sign of the tangential momentum p ; the replacement of an electronlike quasiparticle by a holelike quasiparticle with the same energy and *vice versa* can be ignored, since the simultaneous change of the sign of the charge and the mass does not alter the dynamics. Incorporating the change of the sign of p at the interface into the Poincaré maps (1) and (2) gives

$$\phi_{n+1} = \phi_n + \omega(p_n) \pmod{2\pi}, \quad (4)$$

$$p_{n+1} = p_n \Phi(\phi_n), \quad (5)$$

with

$$\Phi(\phi) = \begin{cases} -1 & \text{if } 0 < \phi < \beta, \\ 1 & \text{otherwise.} \end{cases} \quad (6)$$

The tangential momentum p is no longer a constant of motion, but $|p|$ is. An invariant set $|p| = p_0 > 0$ consists of two circles $p = p_0$ and $p = -p_0$, which are separated in phase space (ϕ, p) . The topology of this situation is schematically

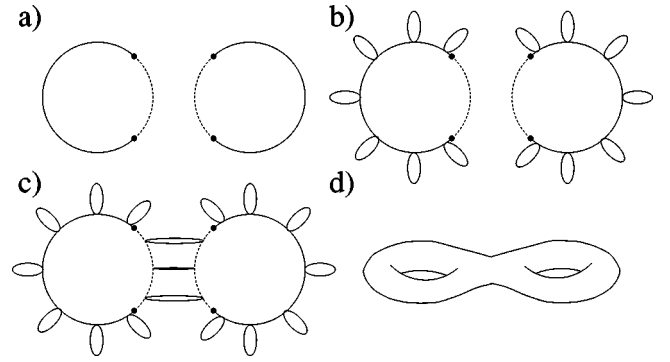


FIG. 3. Construction of the invariant surfaces from the invariant sets. Dotted lines mark the superconducting interface. Thick dots mark the critical points.

illustrated in Fig. 3(a). An invariant surface of the continuous-time dynamics is obtained from the invariant set by attaching circles as shown in the sequences of Figs. 3(a)–3(d). The circles represent the radial motion, which is not contained in the Poincaré map: after leaving the boundary, the radial coordinate decreases until it reaches its minimum; then it increases again until it reaches its maximum at the boundary. At a normal-conducting boundary point, this path is a full loop. Hence, we attach such a circle to each point of the set $\phi \in (\beta, 2\pi)$ and $p \in \{p_0, -p_0\}$ [solid lines in Fig. 3(b)]. At a superconducting boundary point, p changes to $-p$ and we have to trace the path once again to obtain a full loop. Hence, we connect each point $\phi \in (0, \beta)$ and $p = p_0$ with the opposite point $p = -p_0$ [dashed lines in Fig. 3(c)] and *vice versa*. The resulting surface has the topology of a two-handled sphere (genus 2) as illustrated in Fig. 3(d). At the critical points $\phi = 0$ and $\phi = \beta$ the motion is not well defined. Two neighboring orbits hitting the boundary of the billiard at different sides of a critical point separate from each other by moving along different handles of the invariant surface. This is fully analogous to the situation near critical corners in rational polygonal billiards; cf., e.g., [5].

Let us now briefly demonstrate that the situation does not change qualitatively when the quasiparticles are not exact at the Fermi energy, i.e., $\varepsilon > 0$. The electronlike quasiparticle with tangential momentum p_e is reflected in a holelike quasiparticle with $p_h \neq -p_e$. Both particles have different Larmor radius, resulting in a different ω . However, if we redefine the tangential momentum as $\tilde{p} = ap + b$ with $a = 2c/(p_e - p_h)$, $b = -a(p_e + p_h)/2$, $0 < c \leq 1$, and also redefine ω correspondingly then we recover maps (4) and (5). Hence, it is sufficient to consider $\varepsilon = 0$ as we will do in the following.

III. THE ASYMMETRIC BARRIER BILLIARD

Before analyzing maps (4) and (5) in more detail, we discuss an interesting relation to a specific rational polygonal billiard. A particle with unit mass moves freely inside a polygon consisting of a vertical line of length b placed in a rectangle with width $L^- + L^+$ and normalized height 1; see Fig. 4. The symmetric case $L^- = L^+$ with $b = 1/2$ is the usual

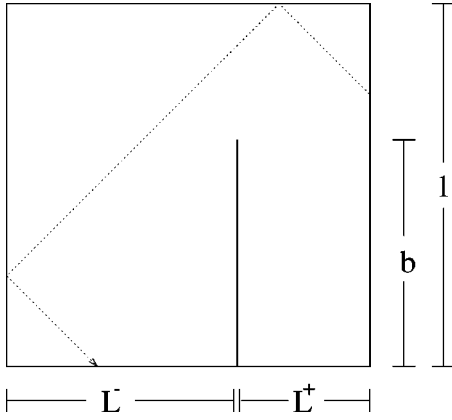


FIG. 4. Asymmetric barrier billiard, rectangle with a vertical line connecting the origin of the coordinate system $(x,y)=(0,0)$ with the point $(x,y)=(0,b)$.

barrier billiard [13–15]; more general cases have been considered in [16–18]. Again, the trivial energy dependence is scaled away by setting the energy to $1/2$, or equally the magnitude of the momentum (p_x, p_y) to 1. Starting with an initial momentum, only a finite number of directions can be achieved during time evolution, stemming from the fact that all angles in the polygon are rational multiples of π . In phase space, the motion takes place on two-dimensional invariant surfaces $(|p_x|, |p_y|) = \text{const}$. The general formula for the genus of such surfaces [5] gives value 2 due to the critical corner at the end of the barrier.

It is convenient to consider the barrier billiard as two rectangular billiards, one with $x \geq 0$ and one with $x \leq 0$, connected by the passage $x=0, y > b$. Suppose for a moment that the passage is closed, $b=1$. For each of the two integrable rectangular billiards we introduce action variables $I_x = |p_x|L/\pi$ and $I_y = |p_y|/\pi$, where L stands for L^- and L^+ . The time dependence of the angle variables is given by $\phi_x(t) = \omega_x t \pmod{2\pi}$ and $\phi_y(t) = \omega_y t \pmod{2\pi}$ with the frequencies $\omega_x = \pi^2 I_x / L^2$ and $\omega_y = \pi^2 I_y$. The flow on the torus is ergodic if and only if the winding number $\rho = \omega_y / \omega_x = I_y L^2 / I_x$ is irrational. When the passage is open, $b < 1$, the particle can move from one rectangle to the other one. We label the rectangles with the sign of $x, s = \pm 1$. We then introduce the Poincaré section $x=0$, i.e., we look at the line in configuration space where $s(t)$ possibly changes. Choosing the origin of the angle variables and the barrier length b such that the passage is given by $0 < \phi_y < \beta = 2\pi(1-b)$, we get the map

$$\phi_{y,n+1} = \phi_{y,n} + 2\pi\rho(s_n) \pmod{2\pi}, \quad (7)$$

$$s_{n+1} = s_n \Phi(\phi_n). \quad (8)$$

Even though the functions $2\pi\rho$ and ω are quite different, maps (7) and (8) are related to the maps (4) and (5) in the following sense. Consider an orbit $(\phi_0, p_0), (\phi_1, p_1), \dots$ in the Poincaré map of the Andreev billiard (4), (5). Denote the two “frequencies” as $\omega^+ = \omega(|p|) \pmod{2\pi}$ and $\omega^- = \omega(-|p|) \pmod{2\pi}$. The family of orbits parametrized by all accessible initial conditions (ϕ_0, p_0) (with fixed ω^+, ω^-) is an

invariant set and related to an invariant surface of the Andreev billiard as described in Sec. II. Consider now an orbit $(\phi_{y,0}, s_0), (\phi_{y,1}, s_1), \dots$ in maps (7) and (8) with $2\pi\rho(+1) = \omega^+$ and $2\pi\rho(-1) = \omega^-$. This can be achieved by constructing a barrier billiard with $L^+ = \omega^+ |p_x/p_y| / (2\pi)$ and $L^- = \omega^- |p_x/p_y| / (2\pi)$ where (p_x, p_y) is the initial momentum. The family of orbits parametrized by all accessible initial conditions $(\phi_{y,0}, s_0)$ [with fixed $(p_x, p_y), L^+$, and L^-] corresponds to an invariant surface of the barrier billiard. The two considered families of orbits are identical if we identify ϕ_y with ϕ , and s with $\text{sign}(p)$. This interesting relation between orbits indicates that invariant surfaces in the circular Andreev billiard not only have the same topology as in the barrier billiard, but also the dynamics on these surfaces (restricted to the chosen Poincaré surfaces of section) have typically the same ergodic properties. We will discuss this issue in detail in the following section. It is to emphasize that for our purpose it is not relevant that this kind of equivalence is not complete (we have ignored the trivial circles lying entirely inside the billiard boundary for $R < 1$) and possibly not bijective (i.e., given a family of orbits in the barrier billiard there may be no counterpart in the Andreev billiard). A complete correspondence between the barrier and circular Andreev billiards is not expected since the former one is symmetric under time reversal whereas the latter one is not.

Note that both maps have four points at which the dynamics is discontinuous, $(\phi_y, s) = (0, \pm 1)$ and $(\phi_y, s) = (\beta, \pm 1)$. In the Andreev billiard these points are two copies of the two critical points; see Fig. 3(a). In the barrier billiard, the points are four copies of the critical corner.

IV. DYNAMICS ON THE INVARIANT SETS

We now discuss the dynamics of the piecewise linear, area-preserving maps (4) and (5) on the invariant sets. Clearly, the dynamics is not chaotic, since all Lyapunov exponents are zero. However, weaker ergodic properties, such as, mixing, weak mixing, and ergodicity may be present. First, ergodicity on the invariant sets follows directly from the fact that an orbit of maps (4) and (5) has a counterpart in maps (7) and (8), which is typically ergodic because the flow on the invariant surfaces in rational polygons is ergodic and not mixing [8]. However, mixing behavior of maps (4) and (5) cannot be excluded with this reasoning. We do this numerically by iterating Eqs. (4) and (5) and computing the time-averaged autocorrelation function (AF)

$$R_z(j) = \frac{\langle z_{n+j} z_n \rangle}{\langle z_n^2 \rangle}, \quad (9)$$

where z stands for $p - \langle p \rangle$ and $\phi - \langle \phi \rangle$, respectively. We have found that the AF typically does not decay to zero, which excludes the mixing property. However, the integrated AF

$$R_{z,\text{int}}(n) = \frac{1}{n} \sum_{j=0}^n |R_z(j)|^2 \quad (10)$$

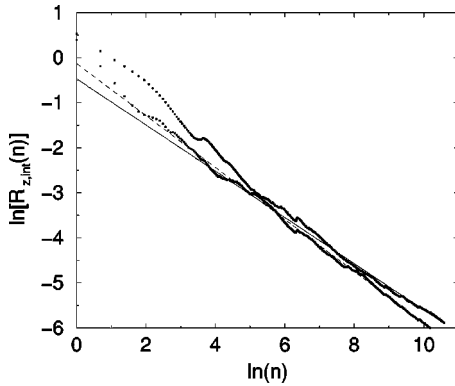


FIG. 5. Integrated autocorrelation function $R_{z,int}(n)$ for $\beta = 1/2$, $R = 1/4$, and $p_0 = 3/4$ in a ln-ln plot: the upper set of points refers to $z = p - \langle p \rangle$ (solid line is the linear fit), while the lower set of points refers to $z = \phi - \langle \phi \rangle$ (dashed line).

is found to vanish according to a power law, n^{-D_2} with $0 < D_2 < 1$ for large n ; D_2 is the correlation dimension of the spectral measure [19]. The example in Fig. 5 shows that the integrated AF for both p_n and ϕ_n clearly obeys the power law with $D_2 \approx 0.513$ and $D_2 \approx 0.577$, respectively. We observe qualitatively identical behavior for several nontrivial functions $f(p_n, \phi_n)$ in a more or less pronounced way, which is consistent with weak mixing as maximal ergodic property.

However, this does not directly imply that the continuous-time evolution is also weak mixing on the invariant surfaces. For example, the barrier billiard in Fig. 4 is not weak mixing since $y(t)$ is a periodic function. Nevertheless, since we cannot find such a trivial component in the continuous-time evolution of the Andreev billiard, we believe that it is weak mixing, but this certainly needs further studies.

From our results we draw the following picture of the motion in configuration space; cf. Fig. 1. Starting with a small cluster of initial conditions with fixed tangential momentum at the boundary away from the superconducting interface, the particles move collectively along skipping trajectories with constant mean angular velocity [$v\omega(p)$ divided by the arclength of the orbits] until the superconducting region is met. Then, the sign of the tangential momentum is inverted. Elementary geometry shows that the mean angular velocity changes. At the next collision with the superconducting region the same thing happens. Orbits reaching the boundary at different sides of a critical point separate after leaving the boundary. Hence, the cluster of initial conditions starts to spread out on the invariant surface. However, weak mixing allows occasional reclusterings with decreasing frequency (the AF does not decay to zero, but the integrated AF does).

Finally, we address the two limiting cases of zero and high magnetic fields. In the zero-field limit, time-reversal symmetry is recovered, $\omega(-p) = -\omega(p)$. All orbits are self-retracing and periodic. The phase space is foliated by periodic orbits rather than by two-dimensional surfaces. In the regime of high magnetic field, $\omega(p)$ is small and close to $\omega(-p)$. This situation corresponds to the symmetric barrier billiard with small ρ .

V. CONCLUSION AND OUTLOOK

We have studied a kind of pseudointegrable system, the circular Andreev billiard. It is different from known pseudo-integrable systems in three respects: (i) it does not belong to the class of polygonal billiards; (ii) it is not symmetric under time reversal; and (iii) it has a nontrivial foliation of energy surfaces by invariant surfaces of genus 2 and two-parameter families of periodic orbits (not touching the billiard boundary). We have shown that the critical points, i.e., the boundary points separating normal and superconducting regions, play the role of critical corners in polygons. Moreover, we have demonstrated that the dynamics on invariant surfaces in the circular Andreev billiard have typically the same ergodic properties as in the asymmetric barrier billiard (restricted to the chosen Poincaré surfaces of section). This finding has been used to show that the Poincaré map is ergodic on the invariant sets. Moreover, we have provided numerical evidence that the Poincaré map is generically weak mixing.

Weak mixing as maximal ergodic property implies interesting spectral properties [20] and anomalous transport. Recent studies in these directions on rational polygons [10,11,16] should be easy to carry over to the circular Andreev billiard.

Of particular interest is the quantum mechanics of the circular Andreev billiard because of two reasons. First, due to the pseudointegrability we expect an exotic quantum-classical correspondence as in rational polygons [15]. Second, as for rational polygons we might observe intermediate energy-level statistics [21], which are, however, modified by the broken time-reversal symmetry and the nontrivial foliation.

The link between the two different classes of systems may also throw some light on one aspect of the proximity effect in chaotic Andreev billiards, viz., the appearance of a gap in the local density of states in an energy interval above the Fermi energy. Random matrix theory can model this gap [22,23], but the semiclassical theory predicts an exponential suppression of the density of states [24,25]. One origin of this discrepancy could be the diagonal approximation used in the semiclassical theory [26]. However, our finding indicates another possible explanation. It is well known that the semiclassical treatment of polygonal billiards requires not only periodic orbits but also diffractive orbits, that is orbits starting and ending at critical corners; see e.g., [27] and references therein. An interesting research project would be to incorporate analogously diffractive orbits (stemming from the critical points) in the semiclassical theory of Andreev billiards and see if this removes the discrepancy to the random matrix theory. This idea is supported by the fact that pointlike scatterers (diffraction) in Andreev billiards gives rise to a gap in the spectrum near the Fermi energy [28].

ACKNOWLEDGMENT

I would like to thank H. Schomerus for useful discussions and critically reading the manuscript.

- [1] M.V. Berry, *Eur. J. Phys.* **2**, 91 (1981).
- [2] A. Andreev, *Zh. Eksp. Teor. Fiz.* **46**, 1823 (1964) [*Sov. Phys. JETP* **19**, 1228 (1964)].
- [3] A. Andreev, *Zh. Eksp. Teor. Fiz.* **49**, 655 (1965) [*Sov. Phys. JETP* **22**, 455 (1966)].
- [4] I. Kosztin, D. Maslov, and P. Goldbart, *Phys. Rev. Lett.* **75**, 1735 (1995).
- [5] P.J. Richens and M. Berry, *Physica D* **2**, 495 (1981).
- [6] A. Hobson, *J. Math. Phys.* **16**, 2210 (1975).
- [7] A. Zemlyakov and A. Katok, *Math. Notes* **18**, 760 (1975).
- [8] E. Gutkin, *J. Stat. Phys.* **83**, 7 (1996).
- [9] V. I. Arnol'd and A. Avez, *Ergodic Problems of Classical Mechanics* (Benjamin-Cummings, Reading, MA, 1968).
- [10] R. Artuso, G. Casati, and I. Guarneri, *Phys. Rev. E* **55**, 6384 (1997).
- [11] R. Artuso, I. Guarneri, and L. Rebuzzini, *Chaos* **10**, 189 (2000).
- [12] J. Blaschke and M. Brack, *Phys. Rev. A* **56**, 182 (1997).
- [13] R. Zwanzig, *J. Stat. Phys.* **30**, 255 (1983).
- [14] J.H. Hannay and R.J. McCraw, *J. Phys. A* **23**, 887 (1990).
- [15] J. Wiersig, *Phys. Rev. E* **64**, 026212 (2001).
- [16] J. Wiersig, *Phys. Rev. E* **62**, R21 (2000).
- [17] G. Zaslavsky and M. Edelman, *Chaos* **11**, 295 (2001).
- [18] A. Eskin, H. Masur, and M. Schmoll, e-print cond-mat math.DS/0107204.
- [19] R. Ketzmerick, G. Petschel, and T. Geisel, *Phys. Rev. Lett.* **69**, 695 (1992).
- [20] I. Cornfeld, S. Fomin, and Y. Sinai, *Ergodic Theory* (Springer, Berlin, 1982).
- [21] E. Bogomolny, U. Gerland, and C. Schmit, *Phys. Rev. E* **59**, R1315 (1999).
- [22] J. Melsen, P. Brouwer, K. Frahm, and C. Beenakker, *Europhys. Lett.* **35**, 7 (1996).
- [23] J. Melsen, P. Brouwer, K. Frahm, and C. Beenakker, *Phys. Scr. T* **69**, 223 (1997).
- [24] A. Lodder and Y. Nazarov, *Phys. Rev. B* **58**, 5783 (1998).
- [25] H. Schomerus and C. Beenakker, *Phys. Rev. Lett.* **82**, 2951 (1999).
- [26] W. Ihra, M. Leadbeater, J. Vega, and K. Richter, *Eur. Phys. J. B* **21**, 425 (2001).
- [27] E. Bogomolny, N. Pavloff, and C. Schmit, *Phys. Rev. E* **61**, 3689 (2000).
- [28] S. Pilgram, W. Belzig, and C. Bruder, *Phys. Rev. B* **62**, 12 462 (2000).